Low Temperature Physics/Fizika Nizkikh Temperatur, 2021, vol. 47, No. 11, pp. 1061–1071

Optical spectroscopy study of $KDy(WO_4)_2$: Crystal-field levels of Dy^{3+} and the Jahn–Teller transition

S. A. Klimin

Institute of Spectroscopy of the Russian Academy of Sciences, Troitsk, Moscow 108840, Russia
E-mail: klimin@isan.troitsk.ru

A. V. Peschanskii

B. Verkin Institute for Low Temperature Physics and Engineering of the National Academy of Sciences of Ukraine Kharkiv 61103, Ukraine

Received July 15, 2021, published online September 24, 2021

Transmission spectra of a double potassium-dysprosium tungstate $KDy(WO_4)_2$ single crystal in the region of intermultiplet transitions of the Dy^{3+} ion and the Raman spectra of light scattering on the electronic levels of the ${}^6H_{15/2}$ ground multiplet of Dy^{3+} are studied in a wide temperature range. The energy scheme for the crystal-field (CF) levels of Dy^{3+} in $KDy(WO_4)_2$ is created. The phase transition at the temperature 6.3 K is accompanied by the lowering of the energy of the ground Dy^{3+} CF state, which is evidenced by both the transmission and Raman spectroscopies. Splitting of the low-lying (~13 cm^{-1}) first excited CF level of the Dy^{3+} ion indicates the simultaneous structural phase transition. The role of Davydov interaction is discussed.

Keywords: $KDy(WO_4)_2$ crystal, Jahn–Teller effect, IR spectroscopy, Raman spectroscopy, Dy^{3+} crystal-field levels.

1. Introduction

Double alkaline-rare-earth compounds from the families of molybdates and tungstates have long been the objects of active research. Interest in these compounds is due to the presence of structural phase transitions (PT) in them and the presence of complex magnetic ordering below 1 K [1–3]. In addition, double tungstates with the general formula $MRE(WO_4)_2$ (M = K, Rb, Cs; RE is a rare-earth ion) can also have important practical applications, since these monoclinic crystals possess good laser properties [4–11]. Monoclinic α-$KRE(WO_4)_2$ tungstates also have large nonlinear optical susceptibilities $\chi^{(3)}$, and therefore can be used in various laser applications based on the phenomena of stimulated Raman scattering [12–16]. But despite a long period of research and a large number of published works, not all the physical properties of these compounds have been fully studied and there are contradictions in the available literature data.

Among the series of double tungstates, the most studied is double potassium-dysprosium tungstate. A spectroscopic study of a $KDy(WO_4)_2$ single crystal showed anomalous shifts of the optical absorption band maxima at a temperature of ~ 10 K [17]. These shifts are associated with an increase in the energy distance between the lowest CF Kramers doublets of the ground term ${}^6H_{15/2}$ of the Dy^{3+} ion during the structural phase transition (from ~ 10 cm^{-1} in the high-temperature phase to ~ 18 cm^{-1} in the low-temperature phase). The discovered phase transition was associated with the cooperative Jahn–Teller effect (CJTE) caused by the electron-phonon interaction of the Dy^{3+} ions [17]. Temperature measurements of the dielectric permittivity ε revealed an anomalous increase in ε with a maximum in the region of the PT temperature ($T_C \sim 10$ K) [18]. The magnitude of the dielectric anomaly ($\Delta\varepsilon \sim 13$ %) significantly exceeds specific values in the measurement for a purely structural phase transition ($\Delta\varepsilon \sim 0.1$–1 %). The authors of [18] interpreted the Jahn–Teller ordering as improper antiferroelectric. In Ref. 19, on the basis of the available data, within the framework of the used CJTE model, it is assumed that the phase transition is accompanied by ferrodistortion ordering of structural deformations and occurs without changing the number of atoms in the unit cell. The structural phase transition $C_{2h}^6 \to C_i^1$ at $T_C \sim 7$ K is accompanied by the appearance of two spontaneous components of the deformation tensor and can be classified as ferroelastic [19].

In Ref. 20, the study of the heat capacity of $KDy(WO_4)_2$ was performed at low temperatures. T_C was determined very accurately as (6.38 ± 0.02) K and it was noted that the deviation from the cubic dependence in the behavior of the heat capacity takes place already in the temperature range $T < 15$ K. Double potassium-dysprosium tungstate orders magnetically at a temperature 0.6 K [21]. A structural phase transition of $KDy(WO_4)_2$ at $T_C = 6.38$ K was confirmed by other experiments, namely, by the temperature dependences of the magnetization, of the linear thermal expansion coefficient, and of the halfwidth of the absorption line [22]. From the angular dependences of the EPR spectra, the values of the g factors of Dy^{3+} were determined in both the high-temperature ($T > 12$ K: $g_x = 0$, $g_y = 0.82$, $g_z = 3.13$) and the low-temperature ($T = 4.2$ K: $g_x = 0$, $g_y = 1.19$, $g_z = 1.98$) phases and it was concluded that the phase transition does not change the symmetry of the initial high-temperature phase, but a smooth distortion of the lattice occurs in the *ac* plane. The direction in which the g factor is maximal lies in the *ac* plane and is deflected by 20° from the *c* axis (by 114° from the *a* axis), the g_y direction coincides with the *b* axis. The study of the EPR spectra of a $KDy(WO_4)_2$ crystal and of a magnetically diluted $KY_{0.99}Dy_{0.01}(WO_4)_2$ ($g_x = 0$, $g_y = 1.54$, $g_z = 14.6$) showed a significant difference in the g factors of the Dy^{3+} ion in the two compounds [23].

Measurements of the magnetostriction in a $KDy(WO_4)_2$ single crystal in the temperature range below the temperature of the Jahn–Teller structural phase transition revealed an abrupt irreversible change in the elastic deformation with an increase of the magnetic field directed along both the *a* and *b* axes of the monoclinic crystal cell [24]. The observed residual deformation is retained after a change in the sign of the magnetic field. The return to the initial state is possible only after thermal cycling with temperatures much higher than T_C. The mechanism of jump-like transitions is explained by the magnetic "softening" of elastic moduli near the structural phase transition [24].

Earlier studies of the Raman spectra of $KDy(WO_4)_2$ [25] were carried out at 2 and 25 K and the main attention was paid to the analysis of vibrational modes. All 36 vibrational excitations predicted by group-theoretical analysis for the high-temperature phase were found and their symmetry was determined. An analysis of the temperature behavior of the scattering spectra indicated that the positional symmetry of the crystal is retained upon the structural phase transition, i.e., the C_2 axis is kept in the position of the Dy^{3+} ion. The detection of three additional phonon lines in the low-temperature phase at 2 K (41.5, 76.7, 182.3 cm^{-1}) and the doubling of the number of lines in the region of the first excited level of the Dy^{3+} ion indicated a doubling of the primitive cell during the phase transition [25]. The lack of detailed measurements of the temperature evolution of the scattering spectra and the lack of information on the electronic states of the Dy^{3+} ion in the region of intermultiplet transitions motivated us to carry out further spectroscopic studies.

In this work, we report on the studies of the transmission spectra of a $KDy(WO_4)_2$ single crystal in the region of intermultiplet optical transitions of the Dy^{3+} ion over a wide temperature range. The results of the study of electronic transitions within the ground $^3H_{15/2}$ multiplet of the Dy^{3+} ion by both IR and Raman spectroscopy methods are also presented.

2. Experiment

Double potassium-dysprosium tungstate $KDy(WO_4)_2$ samples were prepared, cut, and thoroughly polished from a single crystal of good optical quality with natural faceting. For different experiments we used different samples. First sample had a shape of a rectangular parallelepiped with dimensions 3.0 × 2.8 × 2.9 mm, it had the edges being parallel to the orthogonal axes x, y, and z, chosen so that $z \parallel C_2 \parallel b$, $y \parallel a$, and $x \perp y$, z and slightly (within 4°) declined from the *c* axis. Second sample was a non-oriented plane-parallel plate with a thickness of 300 μm. The third sample was the KBr tablet with addition of polycrystalline $KDy(WO_4)_2$. To prepare the last one, we took ~ 30 mg of the polycrystalline $KDy(WO_4)$, thoroughly grinded it in an agate mortar, mixed with ~ 250 mg of optically grade KBr, and pressed in a tablet using standard press form. The effective thickness of evenly distributed substance in potassium-bromide-matrice estimated as ~ 15 μm.

Infrared (IR) studies of transmission spectra were performed in a wide frequency range (3000–15000 cm^{-1}) at different temperatures (2.8–300 K). We used a BRUKER IFS125HR fourier-transform spectrometer. Different beamsplitter/detector configurations were used for different spectral ranges, namely, CaF_2/InSb pair for 3000–10000 cm^{-1} and Visible/Si-diode — for 9000–15000 cm^{-1}. For low-temperature measurements we used both closed-cycle helium optical cryostat CRYOMECH PT403 and bath cryostat with helium vapor evacuation. In the first case, the sample was attached to a cold finger with the use of indium envelope, in the second one — the sample was cooled by a helium vapor in the cryostat shaft. The temperature was controlled by a Scientific Instrument temperature controller.

Raman spectra were excited by the 632.8 nm spectral line of 30 mW He-Ne laser. The light scattered by the sample at angle of 90° was analyzed using a Ramanor U-1000 double monochromator and recorded by a cooled photomultiplier with a photon counting circuit. The sample was placed in special optical cryostats, which made it possible to carry out measurements either at 2 K in superfluid helium, or in a wide temperature range from 5 to 300 K in an exchange gas.

The polarization configuration in Raman spectra is presented in standard notation $k(ij)q$, where k and q are the directions of propagation (x, y, z) of the incident and scattered light with an electric vector **E** along i and j, respectively. The designations ZZ, XY, etc., can be considered as short notation (ij instead of $k(ij)q$), they correspond to specific components of the scattering tensor and indices i and j.

3. Crystal structure of α-$KDy(WO_4)_2$ and Dy^{3+} crystal-field levels

The $KDy(WO_4)_2$ crystal has a structure of the α-$KY(WO_4)_2$ type [26, 27] and belongs to the monoclinic centrosymmetric system C_{2h}^6. There are two main arrangement of this space group, namely, C_{2h}^6-$C2/c$ and C_{2h}^6-$I2/c$, most frequently used by researchers to describe the crystal structure of α-$KY(WO_4)_2$, structural data for $KDy(WO_4)_2$ for $C2/c$ arrangement being given in [28]. While the first one is recommended by the International Crystallographic Union as the standard setting [29], the researchers prefer to use the second one simply from practical convenience as its monoclinic angle is close to 90°. In the $I2/c$ setting, the unit cell has the following parameters: $a = 8.05$ Å, $b = 10.32$ Å, $c = 7.52$ Å, $\beta = 94.13°$, $b \parallel C_2$. The primitive cell contains two formula units. The crystal structure of the monoclinic α-$KY(WO_4)_2$ is shown in Fig. 1 plotted using "Balls & Sticks" software [30]. The crystal structure contains three different types of polyhedra. The tungsten and oxygen atoms occupy 8*f* positions, forming four-coordinated polyhedrons (highly distorted tetrahedra) of C1 symmetry. The K and Y atoms with the C2 local symmetries are placed at 4*e* positions and are six and twelve coordinated, respectively. The Y and K polyhedra have a shape of distorted square octahedra and distorted icosahedrons, respectively. The crystal has a rather pronounced layered structure, the layers are located perpendicular to the C_2 axis. The layers of WO_4 polyhedra lying in the *ac* plane alternate with layers containing YO_6 and KO_{12} polyhedra (see Fig. 1).

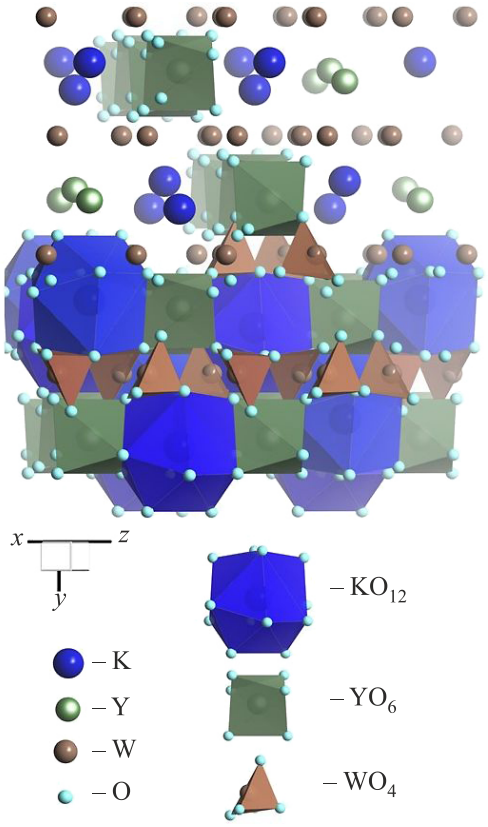

Fig. 1. Crystall structure of α-$KY(WO_4)_2$.

We have to note that we follow the same consideration of yttrium and tungsten polyhedra as was given in Refs. 31, 32 for isostructural $KTb(WO_4)_2$, rather than the consideration of Refs. 28, 33. For example, we consider YO_6 in contrast to YO_8 one, because one pair of bonds in the last one (2×2.711 Å) are much longer than three other pairs (2×2.307 Å, 2×2.304 Å, and 2×2.284 Å). The same situation takes place in the tungsten polyhedron, four distances in the WO_4 polyhedron (1.719 Å, 1.784 Å, 1.84 Å, and 1.93 Å) are much shorter than those for other additional bonds (2.138 Å and 2.355 Å), when the polyhedron WO_6 is taken into account. Moreover, vibrational properties of both $KDy(WO_4)_2$ [25] and isostructural $KTb(WO_4)_2$ [31, 32] are well described in assumption that an isolated WO_4 polyhedron gives its contribution to the phonon spectrum as a separate molecular group.

The Dy^{3+} ions have an electronic configuration $4f^9$ and a large number of $^{2S+1}L_J$ manifolds [34, 35]. In a low-symmetry crystal field of a monoclinic $KDy(WO_4)_2$ matrix (C_S site symmetry) all multiplets are split into $(2J+1)/2$ Kramers doublets which can be split by magnetic field only. The investigation of the CF excitations of the dysprosium ions and of their temperature behavior in a title crystal is the aim of this study.

4. Experimental results

Normalized IR absorption spectrum of the $KDy(WO_4)_2$ crystal in a wide spectral range is shown in Fig. 2. The spectrum consists of several groups of intense spectral lines (optical multiplets) accompanied by high-frequency wings associated with vibronic transitions. Due to the hierarchy of interactions, to which ions with a screened valence *f* shell are subjected in a matrix [35], the crystal field acting on these ions is weak (compared to the spin-orbit interaction), which clearly demonstrates the fact that the energy distances between the multiplets are much larger than the inter-multiplet ones. This property of the *f* ions makes it easy to identify multiplets of rare-earth ions, regardless of the matrix. At the top of Fig. 2, the designations of the $^{2S+1}L_J$ multiplets of the free Dy^{3+} ion are given, the black strokes indicate the positions of the centers of gravity of the multiplets in the compound under study, and the gray ones show, for comparison, the positions of the centers of gravity of Dy^{3+} multiplets in the $LaCl_3$ matrix [35]. Comparison of the energy splitting of multiplets in two matrices, namely, in $KDy(WO_4)_2$ and $LaCl_3$, allows us to conclude that the crystal-field strength in the first matrix is higher than in the second one, but energy shift is due to the so-called nephelauxetic effect [36–38]. The length of the vibronic wings accompanying the multiplets from the high-frequency side is about 1000 cm^{-1}, which is in excellent agreement with the length of the phonon spectrum of $KDy(WO_4)_2$ [25].

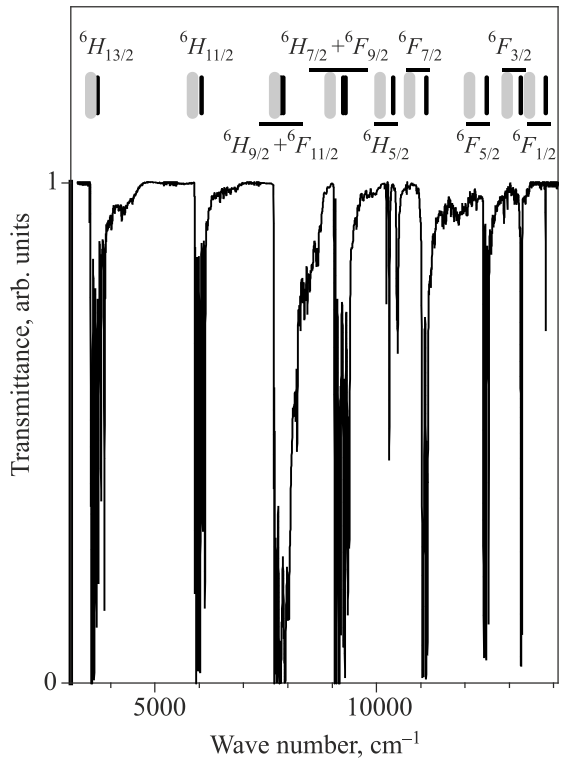

Fig. 2. Normalized absorption spectrum of a 300-μm-thick $KDy(WO_4)_2$ crystal in a wide spectral region at temperature of 4 K. The designation of the Dy^{3+} multiplets is indicated at the top. Black (gray) vertical sticks at the top indicate the gravity center positions of the dysprosium multiplets in $KDy(WO_4)_2$ [this work], (LaF_3 [35]).

Figures 3 and 4 show in detail the spectra in the regions of the transitions from the ground $^6H_{15/2}$ multiplet of the trivalent dysprosium ion in $KDy(WO_4)_2$ to the excited multiplets $^6H_{13/2}$, $^6H_{11/2}$, $^6H_{9/2}$+$^6F_{11/2}$, $^6H_{7/2}$+$^6F_{9/2}$, and $^6H_{5/2}$, $^6F_{7/2}$, $^6F_{5/2}$, $^6F_{3/2}$, $^6F_{1/2}$, respectively, measured at the temperature 5 K. The spectra obtained on the plane-parallel plates of various thicknesses and on the polycrystalline sample are shown. In particular, the dashed lines show the spectra of 2.8 mm thick plane-parallel plate, black lines show the spectra of 300 mm thick plate, and gray lines show the spectra of a polycrystalline sample with an effective thickness of ~ 15 mm. Measurements on samples of different thicknesses are necessary to identify all CF levels, since the intensity of intermultiplet transitions differs by several orders of magnitude. For example, the 2.8 mm thick sample is quite suitable for determining the energies of the Stark levels of the $^6H_{5/2}$ multiplet; at the same time, on this sample, some transitions (for example, $^6H_{9/2}$+$^6F_{11/2}$ and $^6H_{7/2}$+$^6F_{9/2}$) are oversaturated. To determine the energy-level diagram of the latter transitions, a 15 μm thick sample was required.

At the top of each panel shown in Figs. 3 and 4, the energy positions of the CF levels of the Dy^{3+} ion in three isostructural matrices with similar crystal fields are present,

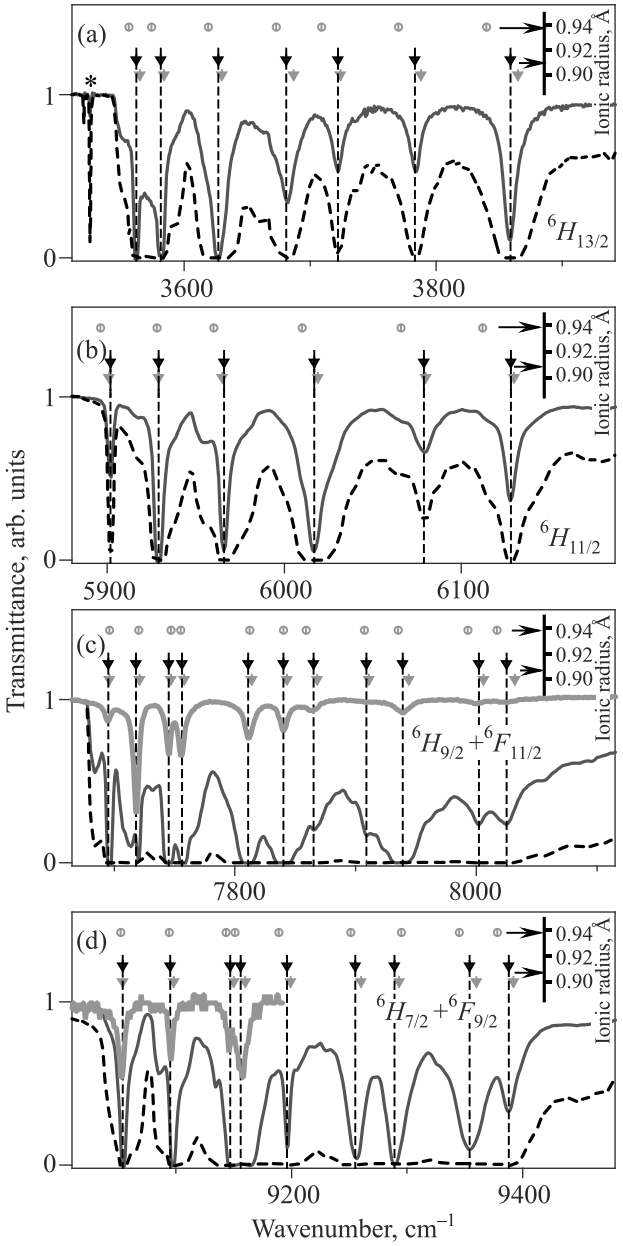

Fig. 3. Transmission spectra of $KDy(WO_4)_2$ at 5 K for (a) $^6H_{13/2}$, (b) $^6H_{11/2}$, (c) $^6H_{9/2}$+$^6F_{11/2}$, and (d) $^6H_{7/2}$+$^6F_{9/2}$ multiplets. Symbols at the top of each panels designate the positions of the Dy^{3+} CF energies in $KGd(WO_4)_2$:Dy^{3+} (gray triangles, from Ref. 33), $KDy(WO_4)_2$ (this work, black triangles), and $KY(WO_4)_2$:Dy^{3+} (gray circles, from Ref. 33), depending on the ionic radius of the main RE^{3+} ion of a given matrix (Gd^{3+}, Dy^{3+}, Y^{3+}). Asterisk marks a weak line belonging to dysprosium in a non-regular site.

namely, $KDy(WO_4)_2$ crystal (black triangles, this work), as well as in $KY(WO_4)_2$ (gray triangles, [33]) and $KGd(WO_4)_2$ (gray circles, [33]). Note also that for many spectral lines, in addition to the main peaks in the $KDy(WO_4)_2$ spectrum, closely spaced wings are observed. This indicates a complex shape of the spectral lines in the concentrated RE compound.

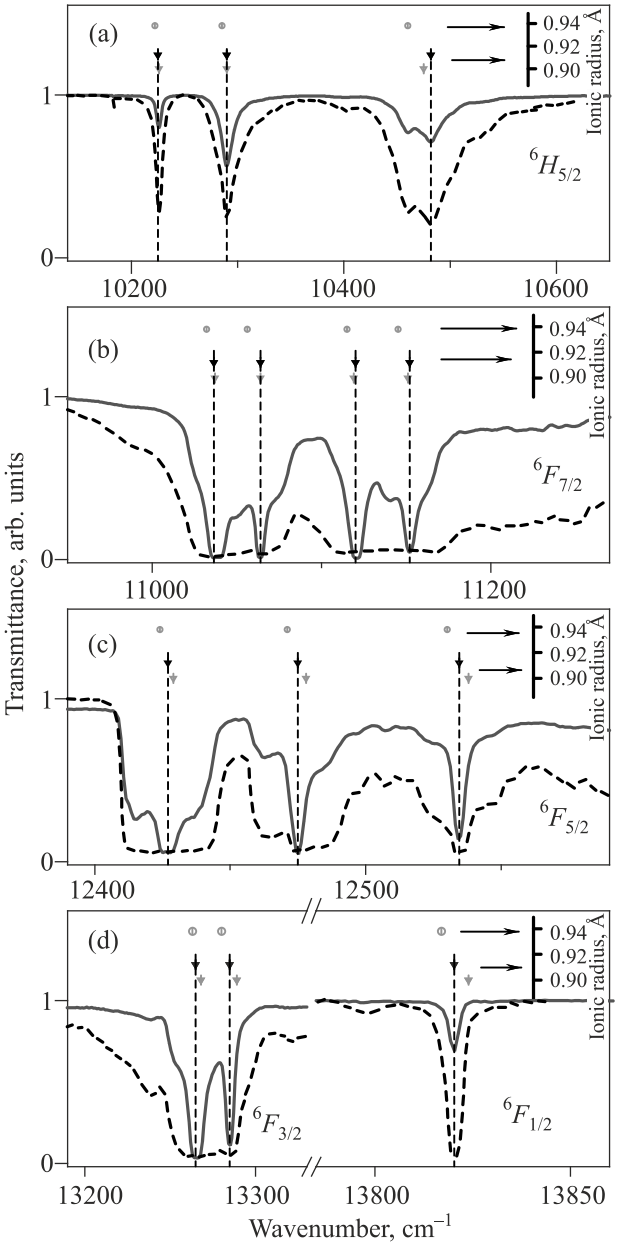

Fig. 4. Transmission spectra of $KDy(WO_4)_2$ at 5 K for (a) $^6H_{5/2}$, (b) $^6F_{7/2}$, (c) $^6F_{5/2}$, and (d) $^6F_{3/2}$ and $^6F_{1/2}$ multiplets. Symbols at the top of each panels designate the positions of Dy^{3+} CF energies depending on the ionic radius of the RE^{3+} ion of given matrix: $KGd(WO_4)_2$ (gray triangles, from Ref. 33), $KDy(WO_4)_2$ (this work, black triangles), and $KY(WO_4)_2$ (gray circles, from Ref. 33).

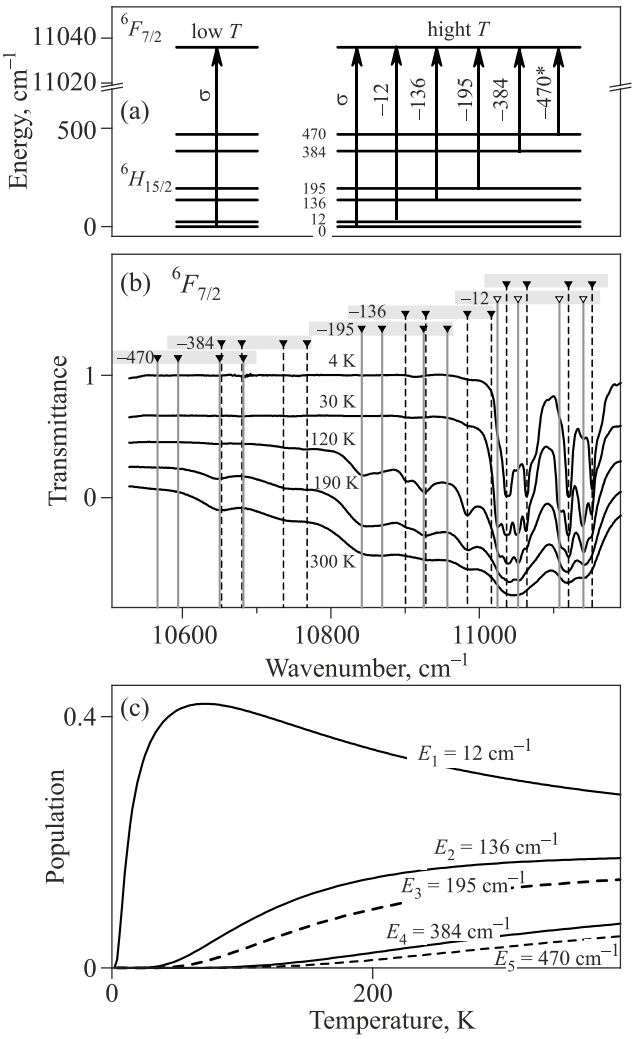

Fig. 5. (a) Schematic presentation of crystal field energies and spectral transitions from ground $^6H_{15/2}$ multiplet to the lowest level of the $^6F_{7/2}$ multiplet at low and elevated temperatures. (b) Transmission spectra for the $^6H_{15/2} \rightarrow {}^6F_{7/2}$ intermultiplet transition at selected temperatures. Symbols at the top of the picture indicate positions for spectral lines determined using the energy level scheme. (c) Temperature behavior of populations for six-level scheme.

Figure 5 shows (a) the scheme of spectral transitions at low and high temperatures, (b) the temperature evolution of the transmission spectra using the example of the $^6F_{7/2}$ multiplet, and (c) the temperature behavior of populations of excited crystal-field levels of the ground $^6H_{15/2}$ multiplet. The general trends in spectral changes with increasing temperature are (i) a broadening of spectral lines, (ii) a decrease in the intensity of "main lines" (transitions from the ground state, which is the only one populated at low temperatures), and (iii) the appearance and growth in intensity of new spectral lines from the low-frequency side of the multiplet, associated with transitions from the excited energy level of the ground $^6H_{15/2}$ multiplet, which are gradually populated with increasing temperature.

Figure 6 shows the Raman spectra of the $KDy(WO_4)_2$ crystal in the low-frequency region in the *ZZ* polarization. Intense lines are due to vibrational modes of the crystal. Their assignment was unambiguously carried out in [25]. At the same time, the spectrum contains weaker lines with a characteristic temperature behavior that differs from the behavior of lines associated with phonons. These lines are marked with arrows in the figure, they broaden significantly with increasing temperature, so much, that at room temperature it becomes impossible to observe them.

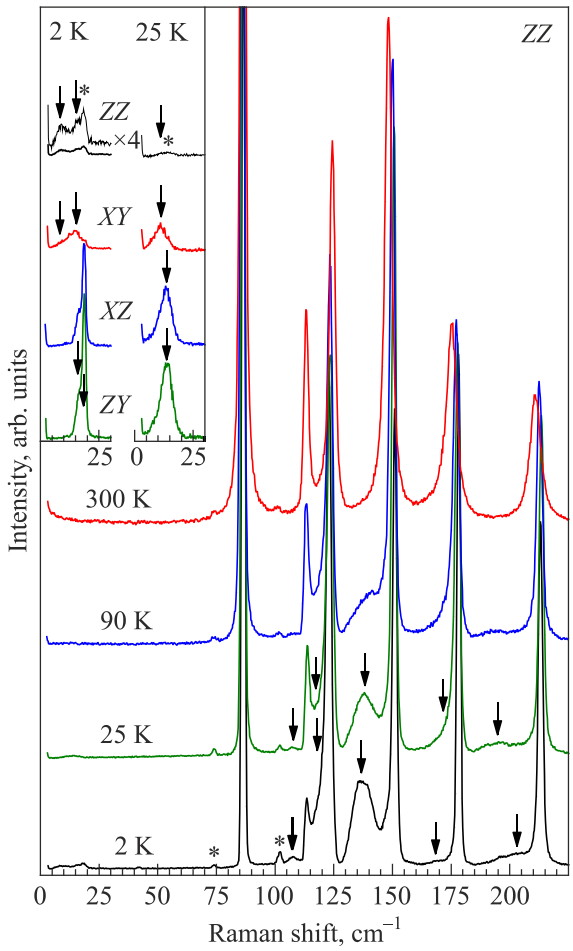

Fig. 6. Temperature behavior of the low-frequency part of the Raman spectra of $KDy(WO_4)_2$ with a *ZZ* scattering tensor component (A_g symmetry). The inset shows spectra at temperatures of 2 and 25 K with different polarizations in the region of the first excited Kramers doublet of the Dy^{3+} ion. The arrows indicate low-energy electronic transitions between the levels of the ground $^6H_{15/2}$ multiplet of the Dy^{3+} ion. Asterisk symbols mark lines that are observed due to depolarization. Spectral resolution is 1.8 cm^{-1} (1.2 cm^{-1} on the inset for *XZ* and *ZY* at 2 K).

5. Discussion

5.1. Energy level scheme

Using the data shown in Figs. 3 and 4, we were able to plot the energy level diagram for the excited multiplets of the Dy^{3+} ion in the $KDy(WO_4)_2$ crystal. For each of the excited multiplets, we were able to find all $2J+1$ energy levels. The obtained data are presented in Table 1, where the comparison with the energies of the Dy^{3+} ion doped into $KY(WO_4)_2$ and $KGd(WO_4)_2$ matrices, taken from the literature data [33], are given. These three matrices are isostructural and have very close crystal-lattice parameters. The three different intrinsic rare-earth ions of the matrices are characterized by slightly different ionic radii. The height at which the symbols in Figs. 3 and 4 are located is proportional to the ionic radius. A similar, practically very close, environment of the Dy^{3+} ion in three matrices means that the crystal field acting on the Dy^{3+} ion and splitting of the free-ion multiplets into CF levels are also practically the same. This is clearly proved by the closeness of the arrangement of spectral lines in all three matrices (see Figs. 3 and 4).

Note that the spectrum contains weak lines of the dysprosium ion that do not belong to the regular center of the Dy^{3+} ion located in the 4*e* position. An example of such line (marked by asterisk) with the frequency of 3525 cm^{-1} is shown in Fig. 3(a). The presence of weak lines for rare-earth ions in irregular positions can have a different nature. Such lines are also observed in the case of other rare-earth crystals, and some of them belong not only to impurity phases, but also to rare-earth ions located in the crystal in a nonregular position [39, 40]. The fact that the crystal has excellent optical quality and was previously characterized by other methods, in particular, its vibrational Raman spectrum does not contain the lines of impurity phases [25], as well as the fact that the line 3525 cm^{-1} demonstrate specific behavior in the temperature range below the temperature of the Jahn–Teller transition in $KDy(WO_4)_2$ (T_C = 6.3 K), lead us to the conclusion that the crystal contains a very small number of nonregular dysprosium centers.

To determine the energy structure of the ground $^6H_{15/2}$ multiplet of the Dy^{3+} ion, we have to analyze the temperature-dependent transmission spectra for various multiplets. An example of such spectra is shown in Fig. 5 for the multiplet $^6F_{7/2}$. This multiplet consists of four Kramers doublets. Accordingly, at a low temperature (4 K), four "main" lines are observed in the spectrum. As the temperature rises, new lines appear. Initially, as the first excited level (12 cm^{-1}) of the ground multiplet is populated, satellites appear, shifted by 12 cm^{-1} to the low-frequency side from each "main" line. The position of the group of these satellites is indicated by the marker "–12" in the scheme of Fig. 5(a).

With increasing the temperature, subsequent levels of the ground multiplet are populated and, in accordance with this, new groups of lines appear in the spectrum. The intensities of the satellites are in accordance with the population of the starting level of transition, described by the Boltzmann distribution. For a system of N levels, the population of the ith level can be determined using the following expression:

$$n_i = \frac{e^{-\frac{E_i}{kT}}}{\left(1+\sum\limits_{j=1\ldots N} e^{-\frac{E_j}{kT}}\right)}, \qquad (1)$$

where n_i is the population of ith CF level, $E_{i,j}$ are their energies, k is the Boltzmann constant.

Table 1. Energies (in cm^{-1}) of the crystal-field levels for $^6H_{13/2}$, $^6H_{11/2}$, $^6H_{9/2}$+$^6F_{11/2}$, $^6H_{7/2}$+$^6F_{9/2}$, $^6H_{5/2}$, $^6F_{7/2}$, $^6F_{5/2}$, $^6F_{3/2}$, $^6F_{1/2}$ multiplets of the Dy^{3+} ion in $KDy(WO_4)_2$ crystal compared to those in $KY(WO_4)_2$:Dy and $KGd(WO_4)_2$:Dy

$KDy(WO_4)_2$ This work	$KY(WO_4)_2$:Dy [33]	$KGd(WO_4)_2$:Dy [33]	$KDy(WO_4)_2$ This work	$KY(WO_4)_2$:Dy [33]	$KGd(WO_4)_2$:Dy [33]
$^6H_{13/2}$			$^6H_{7/2}$+$^6F_{9/2}$		
3562	3565	3556	9054	9054	9052
3581.5	3584	3574	9095	9098	9094
3627	3630	3619	9147	9150	9143
3681	3687	3673	9156	9160	9151
3722	3724	3709	9196	9199	9189
3783	3788	3770	9255	9260	9251
3859	3865	3840	9289	9293	9295
$^6H_{11/2}$			9354	9360	9345
5901.8	5901	5896	9388	9392	9378
5929	5929	5928	$^6H_{5/2}$		
5966	5965	5960	10225	10226	10222
6017	6019	6010	10290	10290	10285
6079	6080	6066	10482	10475	10460
6128	6130	6112	$^6F_{7/2}$		
$^6H_{9/2}$+$^6F_{11/2}$			11036.5	11037	11032
7695	7696	7696	11064	11064	11056
7718	7721	7720	11120	11119	11115
7745	7747	7747	11152	11151	11145
7756	7758	7755	$^6F_{5/2}$		
7811	7814	7812	12427	12429	12424
7840	7843	7840	12475	12478	12471
7865	7868	7859	12534.5	12538	12530
7909	7911	7907	$^6F_{3/2}$		
7939	7944	7935	13265	13268	13263
8002	8006	7993	13285	13289	13280
8025	8032	8017	$^6F_{1/2}$		
			13820.3	13824	13817

Table 2. Symmetries and energies (in cm^{-1}) for low-energy crystal-field levels of the ground $^6H_{15/2}$ multiplet of the Dy^{3+} ion in the $KDy(WO_4)_2$ crystal. The proposed division into doublets is also shown

Symmetry	This work			Literature data	
	Raman		IR	IR	
	T = 2 K	T = 25 K	T = 8 K	[33]	[28]
A_g B_g	9.0, 16.2 16.6, 18.6	11.0 13.6	12 (T = 8 K)	11.5	11
					69
A_g	107.4	107.6		–	
A_g	119.0	118.7		–	
A_g A_g	135.0 140.0	137.9	136 (T = 70 K)	137	129
A_g	168.4	172.7		–	
B_g A_g	199.3 206.0	198.8 195.9	200 (T = 100 K)	198	193
				273	270
				326	332
			384 (T = 190 K)	420	407
			470* (T = 300 K)	512	

Using the spectral dependencies shown in Fig. 5(b) and data for other multiplets, the energies of the following levels of the $^6H_{15/2}$ ground multiplet were determined: 0, 12, 136, 195, 384, and 470 cm^{-1} (see also Table 2). This set of energies was used to calculate the temperature dependences of the level populations of the ground multiplet using Eq. (1), they are shown in Fig. 5(c). The temperature dependences of the intensities of the spectral lines are in excellent qualitative agreement with the dependences shown in Fig. 5(c). Indeed, there is a strong growth of satellites, displaced by 12 cm^{-1} from the main lines, in the temperature range from 4 to 30 K, in the same way as the population of the level with an energy of 12 cm^{-1} grows. The next two groups of peaks with a shift of 136 and 195 cm^{-1} appear and grow strongly in intensity at temperatures between 30 and 120 K, which also agrees with an increase in the population of the corresponding energy levels of the ground multiplet. And, finally, the latter groups of lines appear at temperatures above 120 K together with an increase in the populations of the levels at 384 and 470 cm^{-1}. The energy of the last level was determined with a large error due to strong broadening and spectral line overlap; therefore, in the diagram in Fig. 5(a) and in Table 2 the level 470 cm^{-1} is marked by an asterisk.

The energies of the crystal-field levels of the ground multiplet of a rare-earth ion can be obtained also from the Raman spectra [41–44]. Monochromatic light, interacting with matter, is partially scattered, giving rise to elementary excitations of the crystal, which can be not only phonons, but also magnons and electronic excitations — in this case, we are talking about elementary excitations of the Dy^{3+} ion. The assignment of a given spectral line to one or another type of excitation can be revealed from the temperature behavior of the corresponding spectral components. For example, in the Raman spectra of Fig. 6, several spectral lines are observed (marked by arrows), which broaden with increasing temperature much faster than the lines belonging to the scattering by phonons, and due to their strong broadening, they can no longer be recorded at room temperature. Such tendencies are clearly visible in the example of the strongest of these lines, with a frequency of 135 cm^{-1}. This can also be seen on other lines marked with arrows in Fig. 6. Raman lines with frequencies of 11, 135, and 200 cm^{-1} (at 25 K) give energies of the crystal-field levels of the ground multiplet of the Dy^{3+} ion (see Table 2), in agreement with the data obtained from the transmission spectra presented above. Table 2 gives also a comparison with the data from Refs. 28, 33. Raman lines at 119 and 170 cm^{-1} are also assigned to the scattering on crystal-field levels of the Dy^{3+} ion (4*e* site), based on their temperature behavior and the response of the 119 cm^{-1} level to a magnetic field [25]. Thus, the energies 119 and 170 cm^{-1} relate to the missing two energies for the CF levels of the ground multiplet. Indeed, the ground $^6H_{15/2}$ multiplet of the Dy^{3+} ion consists of eight Kramers doublets. Of these, five excited CF levels determined from the IR absorption spectra (12, 136, 200, 384, and 470 cm^{-1}) are in good agreement with the experimental data for dysprosium in the isostructural $KY(WO_4)_2$:Dy crystal (see Table 2). Thus, the 119 and 170 cm^{-1} excitations observed in the Raman spectra complement the energy scheme of CF levels of the ground multiplet of $KDy(WO_4)_2$. Although the energies of 119 and 170 cm^{-1} do not find confirmation in the literature data, the last ones themselves are contradictory. However, we also do not exclude the possibility that some weak lines may belong to dysprosium in nonregular positions. Most likely, the weak line observed in the Raman spectra, corresponding to the excitation with the energy of 107 cm^{-1} and having insignificant changes in an external magnetic field [25], belongs to such nonregular dysprosium ions.

5.2. *Jahn–Teller transition in* $KDy(WO_4)_2$

Figure 7 shows detailed temperature dependences of the two "main" spectral lines, 13820 cm^{-1} and 5900 cm^{-1} in the transmission spectra of the $KDy(WO_4)_2$ crystal. The intensities of these lines increase with decreasing temperature, as it should be for the main lines. The spectral position of both lines does not change in the temperature range 40 K > T_C > ~6.3 K. However, with decreasing temperature, starting from ~ 6.3 K, both lines shown in Fig. 7 begin to shift towards higher frequencies. This behavior is typical for the entire spectrum of excited multiplets. The shift is slightly different for different lines and averages about 1.5 cm^{-1}. There is a critical temperature below which the entire high-frequency spectrum shifts. Figure 8 shows in detail how the position of the 13820 cm^{-1} spectral line changes with temperature. A linear approximation of the two parts (below and above the critical temperature) of the obtained dependence gives the value of T_C near a temperature of 6.3 K (at the point of intersection of two straight lines). This T_C value is in good agreement with the literature data [20, 22].

Since the position of the spectral lines is determined by the crystal field (the energies of the CF states are solutions of the Schrödinger equation for the crystal-field Hamiltonian), it is obvious that the crystal field undergoes some changes in the temperature range below T_C. Both "point charges" of nearby ions and spatially distributed charges (e.g., covalent bonds) contribute to the crystal field. Any redistribution of charges turns out to be associated with the displacement of atoms in the immediate environment. Indeed, either any displacement of atoms or redistribution of space charges (which indirectly also leads to displacements of atoms) will lead to a change in the crystal field. Thus, we come to the conclusion about some structural changes occurring in the $KDy(WO_4)_2$ crystal at $T < T_C$. The presence of a kink on the curve of Fig. 8 rather indicates the presence of a first-order phase transition. In Ref. 25, at a temperature of 2 K, new phonon modes were found in the Raman spectra that are not related to the C_{2h}^6-*I*2/*c* structure,

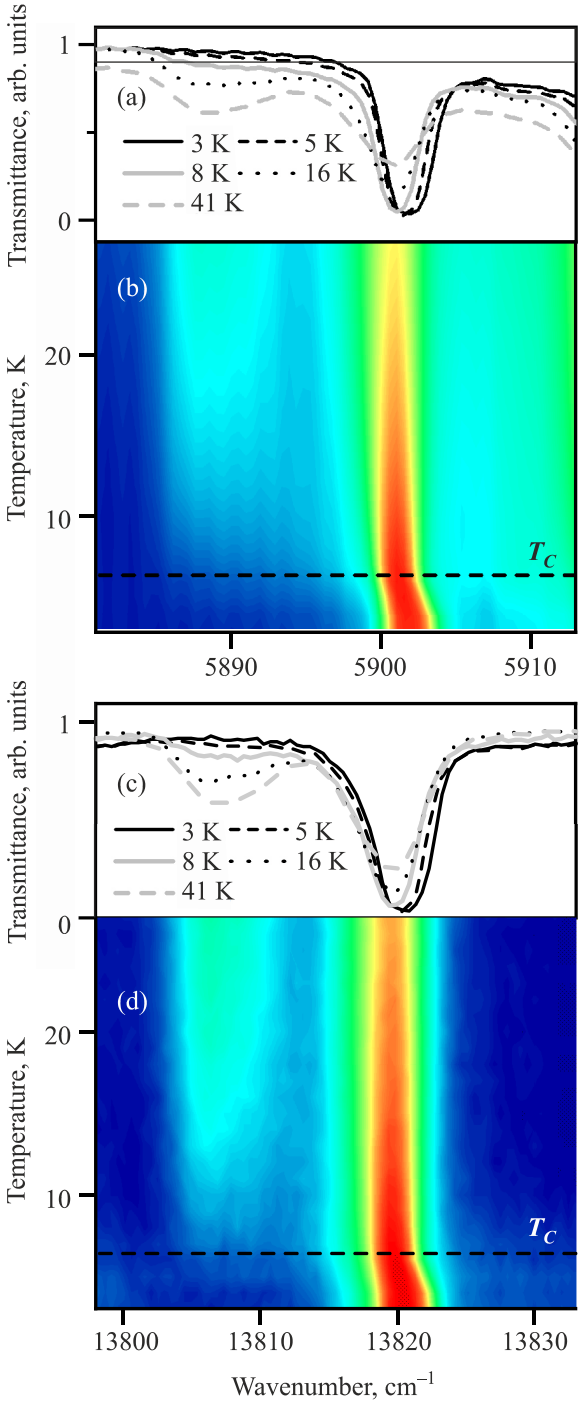

Fig. 7. Transmission spectra of $KDy(WO_4)_2$ at several temperatures. Lines disappearing at low temperatures are due to the transitions originating from excited CF levels of ground multiplet. At temperatures around $T_C = 6.38$ K all spectral lines experience shifts to higher energies. Temperature behavior of spectral lines (a), (b) at 5901 cm^{-1} and (c), (d) at 13820 cm^{-1} shown as (a), (c) spectra at different temperatures and (b), (d) as colored intensity maps.

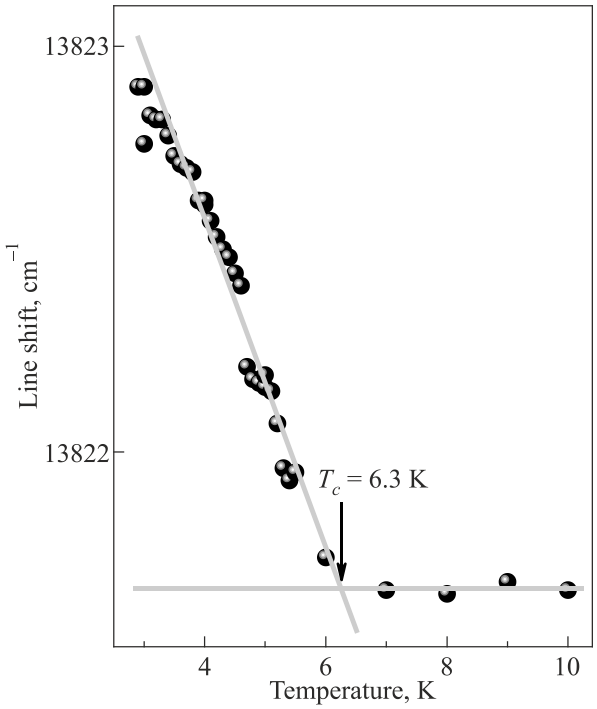

Fig. 8. Temperature behavior of the absorption maximum of the spectral line at 13821.7 cm^{-1} ($^6H_{15/2} \rightarrow {}^6F_{1/2}$). Gray straight lines — root-mean-square linear approximation of experimental data in two temperature ranges: $T > T_C$ and $T < T_C$.

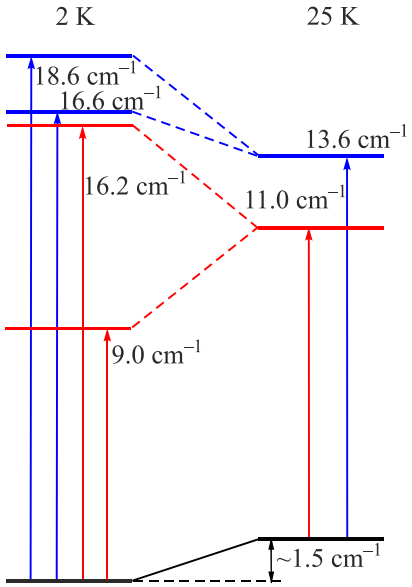

Fig. 9. The level scheme in the region of the first excited Kramers doublet of the Dy^{3+} ion at 2 and 25 K. The crystal-field energies (A_g — red arrows, B_g — blue arrows) were obtained from Raman spectra (Table 2). The value of the shift of the ground state was obtained from the data on IR spectroscopy.

which made it possible to interpret the phase transition at T_C as a change in the crystal structure with a doubling of the unit cell.

Additional information on the change in the spectrum of elementary excitations in the crystal in two phases, at temperatures above and below T_C, was extracted by us from the Raman spectra in the region of low-frequency excitations of the electronic system of the Dy^{3+} ion. The data for the first excited Kramers doublet of dysprosium, given in Table 2, we plotted in the form of a level diagram in Fig. 9.

First, at $T = 25$ K ($T > T_C$) in the spectrum, in the region of the first excited Kramers doublet, there are two excitations, not one. Second, at $T = 2$ K, four excitations are already observed. Third, in the diagram, we have schematically depicted a decrease in the energy of the ground-state level. We made this conclusion on the basis of the data obtained from the analysis of the temperature-dependent transmission spectra. As mentioned above, all spectral lines in the absorption spectra of the $KDy(WO_4)_2$ crystal at $T < T_C$ are shifted to the high-frequency region. The shift of the entire spectrum towards high energies means, obviously, that the energy of the ground state of the Dy^{3+} ion decreases. Thus, the spectroscopic data of this work on the temperature behavior of the energy spectrum of the Dy^{3+} ion indicate that structural changes occur in the crystal due to a decrease in the energy of the rare-earth ion. This is precisely what is implied when considering the Jahn–Teller effect [45]. The state with reduced energy of the rare-earth subsystem is more favorable, but to achieve such situation, a structural shift is required, for the implementation of which the energy costs must be less than the gain obtained by the rare-earth subsystem.

The reason for the decrease in energy are interionic interactions in the dysprosium subsystem, which are possible only in a concentrated rare-earth system. That is why the phase transition under consideration is called the cooperative effect [46]. The presence of interionic interactions is also indicated by the complex shape of the lines in the transmission spectra (see, for example, the shape of the lines at 10482, 11064, 12475 cm^{-1} in Fig. 3). A probable explanation for the presence of two excitations in the region of the first excited Kramers doublet (Fig. 9) can be the Davydov splitting arising from the interaction of two dysprosium ions in the primitive unit cell. The doubling of the unit cell proposed in [25] can also explain the doubling of the number of excitations in the region of the first excited Kramers doublet of dysprosium.

6. Conclusion

Comprehensive studies of the $KDy(WO_4)_2$ crystal was performed by means of Raman and IR transmission spectroscopy in wide temperature and spectral ranges, namely, from room temperature to 2 K, and from THz (< 9 cm^{-1}) to visible (> 14000 cm^{-1}) energy range. A diagram of the Dy^{3+} crystal-field energy states was created. Jahn–Teller transition at $T_C = 6.3$ K was registered by an abrupt shift of infrared and visible CF transitions to the high-energy side. We interpret this as a lowering of the ground CF state of the Dy^{3+} ion arising due to cooperative interion interactions in the Dy subsystem. Interion interaction is proved by existence of two energy states for the first dysprosium CF excitation registered by Raman spectroscopy (modes 11.0 cm^{-1} — A_g and 13.6 cm^{-1} — B_g at 25 K) which was tentatively assigned to Davydov splitting between two dysprosium ions in a primitive cell. The further splitting of this CF excitation into four modes (9.0 and 16.2 cm^{-1} — A_g, 16.6 and 18.6 cm^{-1} — B_g modes at 2 K) proves the presence of structural phase transition previously reported in literature.

1. M. T. Borowiec, V. P. Dyakonov, A. Jedrzejczak, V. I. Markovich, H. Szymczak, E. E. Zubov, and M. Zaleski, *Phys. Lett. A* **243**, 85 (1998).
2. V. P. D'yakonov, V. I. Markovich, V. L. Kovarskii, A. V. Markovich, M. Borowiec, A. Jedrzejczak, and H. Szymczak, *Fiz. Tverd. Tela (St. Petersburg)* **41**, 491 (1999) [*Phys. Solid State* **41**, 440 (1999)].
3. M. Borowiec, V. P. Dyakonov, A. Jedrzejczak, V. I. Markovich, and H. Szymczak, *J. Low Temp. Phys.* **110**, 1103 (1998).
4. A. A. Kaminskii, H. R. Verdun, W. Koechner, F. A. Kuznetsov, and A. A. Pavlyuk, *Kvant. Electron*. (*Moscow*) **9**, 941 (1992) [*Sov. J. Quantum Electron.* **22**, 875 (1992)].
5. M. C. Pujol, M. Rico, C. Zaldo, R. Sole, V. Nicolov, X. Solans, M. Aguilo, and F. Diaz, *Appl. Phys. B* **68**, 187 (1999).
6. A. A. Kaminskii, P. V. Klevtsov, L. Li, and A. A. Pavlyuk, *IEEE J. Quantum Electron.* **8**, 457 (1971).
7. A. A. Kaminskii, P. V. Klevtsov, and A. A. Pavlyuk, *Phys. Status Solidi A* **5**, 79 (1971).
8. A. A. Kaminskii, L. Li, A. V. Butashin, V. S. Mironov, A. A. Pavlyuk, S. N. Bagayev, and K. Ueda, *Jpn. J. Appl. Phys.* **36**, L 107 (1997).
9. A. Kaminskii, U. Hömmerich, D. Temple, J. T. Seo, K. Ueda, S. Bagayev, and A. Pavlyuk, *Jpn. J. Appl. Phys.* **39**, L 208 (2000).
10. A. M. Ivanyuk, P. A. Shachverdov, V. D. Belyev, M. A. Ter-Pogosyan, and V. L. Ermolaev, *Opt. Spectrosk.* (*USSR*) **59**, 950 (1985) [*Opt. Spectrosc.* **58**, 589 (1985)].
11. K. Andryunas, Vishchakas, V. Kabelka, I. V. Mochalov, A. A. Pavlyuk, G. T. Petrovskii, and V. Syrus, *Zh. Eksp. Teor. Fiz. Pis'ma* **42**, 33 (1985) [*Sov. Phys. JETP* **42**, 410 (1985)].
12. K. A. Stankov and G. Marawsky, *Appl. Phys. B* **61**, 213 (1995).
13. J. T. Murray, R. C. Powell, and N. Peyghambarian, *J. Lumin.* **66–67**, 89 (1996).
14. A. A. Kaminskii, K. Ueda, H. J. Eichler, J. Findeisen, S. N. Bagayev, F. A. Kuznetsov, A. A. Pavlyuk, G. Boulon, and F. Bourgeois, *Jpn. J. Appl. Phys.* **37**, L 923 (1998).
15. J. Findeisen, H. J. Eichler, and A. A. Kaminskii, *IEEE J. Quantum Electron.* **35**, 173 (1999).
16. A. A. Lagatsky, A. Abdolvand, and N. V. Kuleshov, *Opt. Lett.* **25**, 616 (2000).
17. I. V. Skorobogatova and A. I. Zvyagin, *Fiz. Nizk. Temp.* **4**, 800 (1978) [*Sov. J. Low Temp. Phys.* **4**, 381 (1978)].
18. L. N. Pelikh and A. A. Gurskas, *Fiz. Tverd. Tela* (*Leningrad*) **21**, 2136 (1979) [*Sov. Phys. Solid State* **21**, 1223 (1979)].
19. I. V. Skorobogatova and E. M. Savchenko, *Fiz. Nizk. Temp.* **6**, 240 (1980) [*Sov. J. Low Temp. Phys.* **6**, 115 (1980)].
20. M. Borowiec, V. P. D'yakonov, A. Jedrzejczak, V. I. Markovich, A. A. Pavlyuk, and H. Szymczak, *Fiz. Tverd. Tela* (*St. Petersburg*) **38**, 2232 (1996) [*Phys. Solid State* **38**, 1229 (1996)].

21. M. T. Borowiec, V. P. Dyakonov, A. Nabialek, A. Pavlyuk, S. Piechota, A. Prokhorov, and H. Szymczak, *Physica B* **240**, 21 (1997).
22. V. P. D'yakonov, V. I. Markovich, V. L. Kovarskii, A. V. Markovich, M. Borowiec, A. Jedrzejczak, and H. Szymczak, *Fiz. Tverd. Tela* (*St. Petersburg*) **40**, 750 (1998) [*Phys. Solid State* **40**, 691 (1998)].
23. I. M. Krygin, A. D. Prokhorov, V. P. Dyakonov, M. T. Borowiec, and H. Szymczak, *Fiz. Tverd. Tela* (*St. Petersburg*) **45**, 1982 (2003) [*Phys. Solid State* **45**, 2083 (2003)].
24. I. B. Krynetskii, A. F. Popkov, A. I. Popov, M. T. Borowiec, A. Nabiałek, T. Zayarnyuk, and H. Szymczak, *Fiz. Tverd. Tela* (*St. Petersburg*) **48**, 1467 (2006) [*Phys. Solid State* **48**, 1553 (2006)].
25. A. V. Peschanskii, *Fiz. Nizk. Temp.* **39**, 1248 (2013) [*Low Temp. Phys.* **39**, 973 (2013)].
26. P. V. Klevtsov and L. P. Kozeeva, *Dokl. Akad. Nauk SSSR* **185**, 571 (1969) [*Sov. Phys. Dokl.* **17**, 185 (1969)].
27. S. V. Borisov and R. F. Klevtsova, *Kristallografiya* **13**, 517 (1968) [*Sov.* Phys. Crystallogr. **13**, 420 (1968)].
28. L. Macalik, J. Hanuza, B. Macalik, W. Ryba-Romanowski, S. Golab, and A. Pietraszko, *J. Lumin.* **79**, 9 (1998).
29. *International Tables for Crystallography*, T. Hanh (ed.), Reidel, Dordrecht (1992), Vol. A.
30. T. C. Ozawa and Sung J. Kang, *J. Appl. Cryst.* **37**, 679 (2004).
31. V. V. Eremenko, V. S. Kurnosov, A. V. Peschanskii, V. I. Fomin, and E. N. Khats'ko, *Fiz. Nizk. Temp.* **33**, 1206 (2007) [*Low Temp. Phys.* **33**, 915 (2007)].
32. A. V. Peschanskii, V. I. Fomin, and A. V. Yeremenko, *Fiz. Nizk. Temp.* **38**, 616 (2012) [*Low Temp. Phys.* **38**, 481 (2012)].
33. A. A. Kaminskii, J. B. Gruber, S. N. Bagaev, K. Ueda, U. Hömmerich, J. T. Seo, D. Temple, B. Zandi, A. A. Kornienko, E. B. Dunina, A. A. Pavlyuk, R. F. Klevtsova, and F. A. Kuznetsov, *Phys. Rev. B* **65**, 125108 (2002).
34. M. A. Elyashevich, *Spectra of Rare Earths Gosttekhteorizdat*, Moscow (1953), also see, the translation USEAC, AEC-tr-4403, Office of Technical Information, Department of Commerce, Washington, DC (1961).
35. G. H. Dieke, *Spectra and Energy Levels of Rare Earth Ions in Crystals*, Wiley, New York (1968).
36. E. Antic-Fidancev, *J. Alloys Compd.* **300–301**, 2 (2000).
37. P.-H. Haumesser, R. Gaumé, B. Viana, E. Antic-Fidancev, and D. Vivien, *J. Phys.*: *Condens. Matter* **13**, 5427 (2001).
38. B. Z. Malkin, A. R. Zakirov, M. N. Popova, S. A. Klimin, E. P. Chukalina, E. Antic-Fidancev, Ph. Goldner, P. Aschehoug, and G. Dhalenne, *Phys. Rev. B* **70**, 075112 (2004).
39. M. N. Popova, E. P. Chukalina, S. A. Klimin, and M. C. Chou, *Quantum Electronics* **50**, 256 (2020).
40. M. A. Kashchenko and S. A. Klimin, *Opt. Spectrosc.* **116**, 836 (2014).
41. V. Peschanskii, *Fiz. Nizk. Temp.* **43**, 1647 (2017) [*Low Temp. Phys.* **43**, 1315 (2017)].
42. D. Fausti, A. A. Nugroho, P. H. M. van Loosdreht, S. A. Klimin, and M. N. Popova, *Phys. Rev. B* **74**, 024403 (2006).
43. A. V. Peschanskii, V. I. Fomin, I. A. Gudim, *Fiz. Nizk. Temp.* **42**, 607 (2016) [*Low Temp. Phys.* **42**, 475 (2016)].
44. S. A. Klimin and M. N. Popova, *EPJ Web of Conferences* **132**, 03021 (2017).
45. I. B. Bersuker, *The Jahn–Teller Effect and Vibronic Intemctions in Modern Chemistry*, Plenum Press, New York (1984).
46. M. D. Kaplan and B. G. Vekhter, *Cooperative Phenomena in Jahn–Teller Crystals*, Plenum, New York (1995).

Оптична спектроскопія кристала $KDy(WO_4)_2$: рівні іона Dy^{3+}, що розщеплені кристалічним полем, та перехід Яна–Теллера

S. A. Klimin, A. V. Peschanskii

Досліджено спектри пропускання Яна–Теллерівського монокристалу подвійного калійдиспрозійового вольфрамату $KDy(WO_4)_2$ в області міжмультиплетних переходів іона Dy^{3+} та спектри раманівського розсіювання світла на електронних рівнях основного мультиплету $^6H_{15/2}$ іона Dy^{3+} у широкому діапазоні температур. Побудовано енергетичну схему для рівнів іона Dy^{3+} в $KDy(WO_4)_2$, що розщеплені кристалічним полем. Фазовий перехід при температурі 6.3 К супроводжується зниженням енергії основного стану іона Dy^{3+}, що підтверджується спектроскопією ІЧ-пропускання та раманівським розсіюванням світла. Розщеплення низьколежачого (~ 13 $см^{-1}$) першого збудженого рівня іона Dy^{3+} вказує на структурний фазовий перехід. Обговорюється роль Давидівської взаємодії.

Ключові слова: $KDy(WO_4)_2$, ефект Яна–Теллера, ІЧ-спектроскопія, раманівська спектроскопія, штарківські рівні.